# The radio emission of the supernova remnants CTB1 and the Cygnus Loop

Dickel, J.R.; Willis, A.G.

Astron. Astrophys. 85, 55–65 (1980)

ASTRONOMY AND ASTROPHYSICS

# The Radio Emission of the Supernova Remnants CTB1 and the Cygnus Loop

J. R. Dickel* and A. G. Willis**
Sterrewacht Leiden, Postbus 9513, NL-2300 RA Leiden, The Netherlands

Received May 7, 1979

**Summary.** High resolution radio maps of CTB1 at 49- and 21-cm wavelengths and of the Cygnus Loop at 49-cm show fine filamentary structures which coincide perfectly with the optical features seen in these SNR. In CTB1, the radio shell is resolved; although the radio features occur within the same region as the optical ones, they fill a larger volume. By comparison of the radio, optical, and X-ray emission from the Cygnus Loop, we investigate a possible mechanism to provide the compression and maintenance of the magnetic field and relativistic particles necessary to produce the radio emission in old SNR. Material which is heated an compressed by passage of the SNR shock through it, will progressively cool behind the shock and the compression of this material to maintain a pressure balance will greatly increase the radio emissivity. Differences between the remnants are attributed to different ambient conditions in their surroundings which create variations in the amounts of heating and compression.

**Key words:** SNR – synchrotron radiation – radio structure

## I. Introduction

The supernova remnants of CTB1 (G116.9+0.1) and the Cygnus Loop (G74.0−8.5) both appear to be relatively old SNR with well defined, although incomplete, optical shells and prominent radio emission. The two objects are somewhat different optically with the Cygnus Loop being composed of very sharp filaments whereas the features in CTB1 are more diffuse (van den Bergh et al., 1973). The Cygnus Loop is also a strong X-ray source with an apparently thermal spectrum representing gas at a temperature of $2–4\,10^6$ K (summarized in Stark and Culhane, 1978). CTB1 is undetected with X-rays but its large distance from the earth allows little meaning to be given to the upper limit for its emmisivity of $13\,10^{35}$ erg s$^{-1}$ in the 1–7 keV range (Gronenschild, 1979). In addition, CTB1 appears to be on the western edge of a broad extended component with a thermal spectrum (Willis and Dickel, 1971) and parts of the Cygnus Loop appear to be interacting with clouds of neutral hydrogen (DeNoyer, 1975).

In both cases there is a general correlation of the radio and optical features (Moffat, 1971; DeNoyer, 1974; Willis, 1973) but the detailed radio shapes and the match of individual filaments have not yet been determined. To do this and, for the Cygnus Loop, to search for the radio counterpart to a faint outer shell to the north seen in Hα (Gull et al., 1977) we have observed these remnants with the Westerbork synthesis radio telescope at a wavelength of 49 cm. The approximately 1′ synthesized beam has provided a resolution of about 1/90 the diameter of the Cygnus Loop, for which our map covers only the area centered on the bright northeastern arc of the shell, NGC 6992. The data extend far enough southward to include the somewhat more diffuse filaments NGC 6995 as well. CTB1, a smaller source, has been observed also at a wavelength of 21 cm where the 23″ beam is again about 1/90 the diameter of the remnant. The equipment and observations are described in Sect. II, the properties of the remnants are given in Sect. III, and a discussion of the results is in Sect. IV.

*Send offprint requests to:* A. G. Willis
* Permanent address: Astronomy Department, University of Illinois, Urbana, Ill. 61801, USA
** Present address: Radiosterrenwacht Westerbork, Schattenberg 4, NL-9433 TA Zwiggelte, The Netherlands

## II. Observations

### A. Equipment

At the time of the observations, the Westerbork telescope consisted of 10 fixed and 2 movable 25-m paraboloids operating in the aperture synthesis mode (see e.g., Högbom and Brouw, 1974). A total of four 12-h-observing runs at different positions for the movable telescopes produces a series of baselines spaced by 18 m from 36 m out to a maximum spacing of 1458 m. The beam patterns synthesized from these observations had the properties given in Table 1. The integration of $4 \times 12^h$ gave the point-source sensitivities shown in the table but, for both fields, the detection of large scale structures on the maps is limited to the second values given because confusion noise and ripple from the grating responses of the various emission features on the maps themselves restrict the dynamic range available. The feeds contain crossed dipoles which can be used to measure the polarization of the incoming radiation.

### B. Results

#### 1. CTB1

The contour maps of CTB1 at 21- and 49-cm wavelengths are shown in Fig. 1a and b and visual representations (or radiophotos) of these maps are presented in Fig. 2a and b. Because the 0 and 18 m spacings are missing in an otherwise uniform coverage of the $U-V$ plane, the synthesized map has both a uniform zero offset and superimposed upon this a small sinusoidal amplitude fluctuation. These effects are particularly noticeable in CTB1 because

**Table 1.** System parameters

| Source | Wavelength (cm) | Declination (°) | HPBW (″) | | Radius of first grating ring (′) | | rms noise level | Detection level for extended structures |
|---|---|---|---|---|---|---|---|---|
| | | | RA | DEC | RA | DEC | (mJy/beam) | |
| CTB1 | 21 | 62 | 22 | 25 | 40 | 46 | 0.15 | 0.5 |
| CTB1 | 49 | 62 | 56 | 64 | 92 | 104 | 0.8 | 3 |
| Cygnus Loop | 49 | 32 | 56 | 107 | 92 | 176 | 0.8 | 4 |

of the emission from the very extended H II region in the field. Because the offset and ripple are contained within the antenna patterns, local values, to some degree, must reflect the whole source structure, but to roughly correct the maps, we have added small constant values of 0.40 and 3.25 mJy to the 21- and 49-cm maps respectively. These represent reasonable estimates for the mean offset within each map field as determined from the total flux densities measured on lower resolution maps (Willis and Dickel, 1971). The ripple appears to have mean amplitudes of approximately 0.5 and 2.5 mJy at 21- and 49-cm respectively. It is apparently mostly contribution from the extended H II region which is quite smooth and so has more flux density in the 18-m spacing at the longer wavelength with its correspondingly larger angular pattern. At 49 cm, the effect is near the noise level but just visible as a slight decrease on the western side of the map and a rise on the northeast. At 21 cm, where the overall flux density of the SNR is lower and the ripple has a higher angular frequency, the fluctuation is more pronounced; the region just inside the bright western part of the source lies in a slight depression and a rise is visible in the northeast.

The bright source Cas A lies only about 5° from our field center on CTB1. It is easily detected at 49 cm although strongly attenuated by the primary beam polar pattern (Willis, in Dickel, 1978). With the 18-m increment in telescope spacing at this wavelength, CTB1 lies between, and thus is not affected by the grating rings. At 21 cm the greater primary beam attenuation reduced the effect of Cas A to a very low level. No grating response is visible above the noise level on the contour map in Fig. 1a, but a faint arc at a level of about 0.1 mJy/beam running diagonally across the center from north-northwest to south-southeast is discernable on an enhanced radiophoto of the whole field.

The final maps of CTB1 shown in Figs. 1 and 2 have been cleaned to remove the spurious responses of the dirty antenna pattern and also the relative brightnesses across the map have been corrected for primary beam attenuation. Finally, the responses of three strong point sources have been subtracted from the 49-cm map and an additional five more from the 21-cm map. The positions of these sources are indicated by asterisks on the contour maps and the sources are also so labeled in Table 2 where

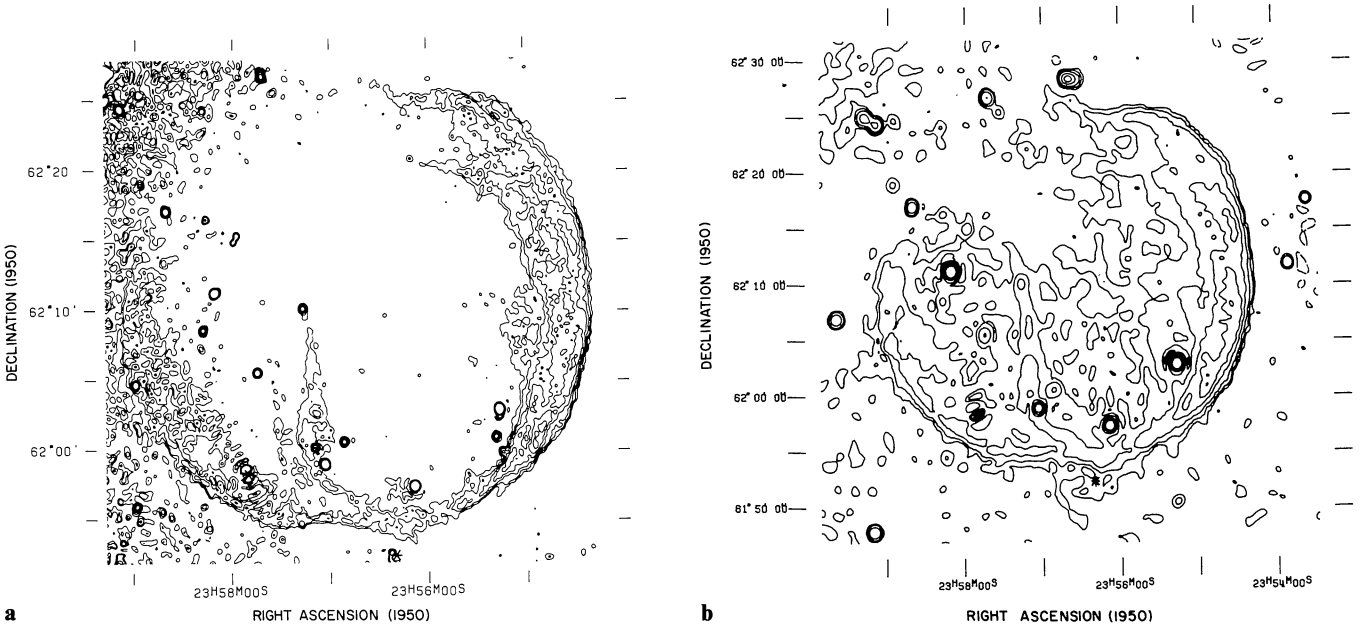


**Fig. 1a and b.** Contour maps of the radio emission from CTB1. The positions where point source have been subtracted are indicated by asterisks. The resolution and shape of the synthesized beam can be seen from the contours of the remaining point sources in the field. **a** 21 cm map. The contour values are 1.5, 2.25, 3.25, 4.5, 6.0, and 7.75 mJy/beam area. **b** 50 cm map. The contour values are −3.75 (dashed), 3.75, 7.5, 15, 30, 45, and 60 mJy/beam area

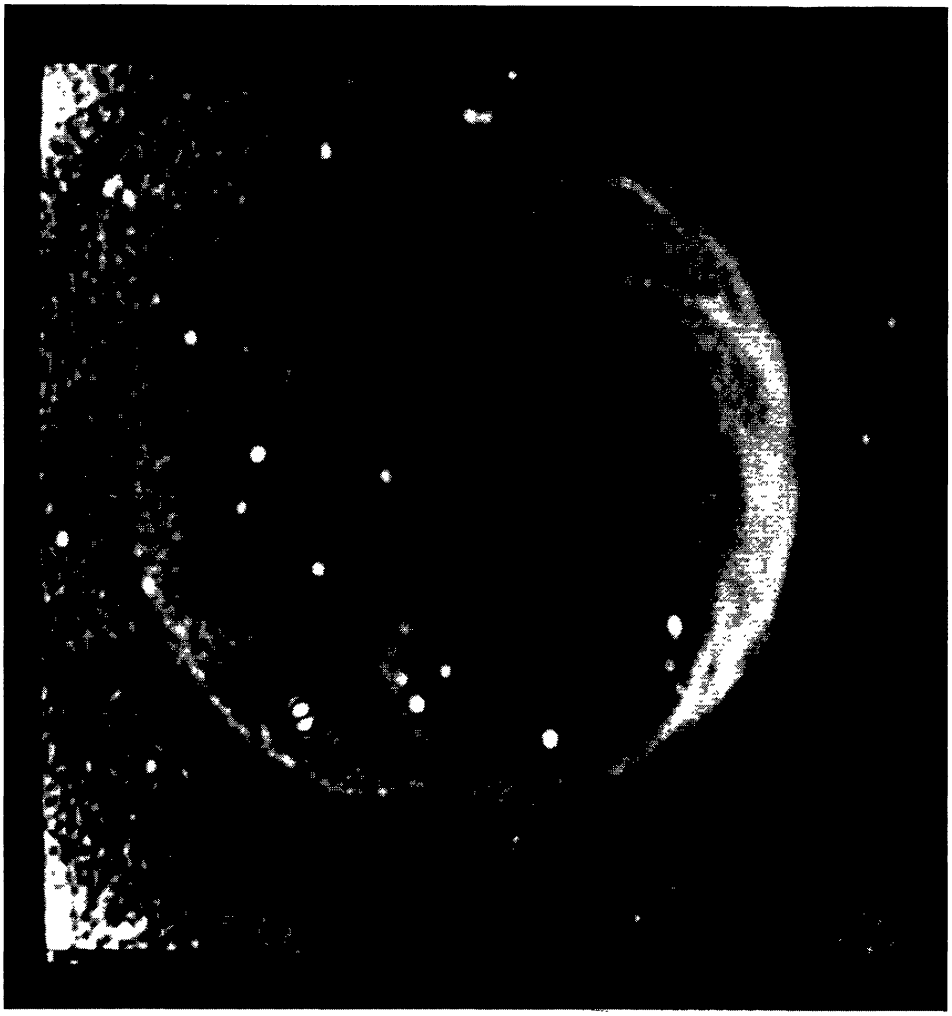

Fig. 2a

**Fig. 2a and b.** Radio photos of the maps of CTB1 shown in Fig. 1: **a** 21 cm, **b** 49 cm

the particulars of all sources in a 1° field centered on the SNR are given. One source which was subtracted was located at $00^h01^m00^s.38$ and 62°31′48″.5, outside the field covered in the table. As can be seen on the maps, the source at $23^h57^m50^s.71$ does not subtract perfectly at either wavelength indicating that it is extended. There is nothing present at this position on the optical photographs of CTB1 (van den Bergh et al., 1973); we suspect it is an unidentified background radio source.

No polarization associated with the remnant was detected above the noise level at either wavelength. This means that, at 21 cm, the polarization of the shell is less than about 10% and that the brightest area on the western side is less than 5% polarized. Limited polarization measurements at a wavelength of 11 cm (Willis and Dickel, 1971; Velusamy and Kundu, 1974) show the peak to have a polarization of perhaps 5% and other areas to be around 10% polarized. Some Faraday depolarization would be expected between 11 and 21 cm so the results are consistent but provide no new information on the polarized component.

## 2. Cygnus Loop

This SNR is very extended – over 3 degrees in diameter – so that we were able to map only a small part of the remnant in a Westerbork field. For best sensitivity and comparison with data at other wavelengths we chose to center our beam on the bright northeastern arc of this remnant, which is the nebulosity designated NGC 6992.

The large extent of the SNR means that there are strong contributions to the brightness at 0- and 18-m spacings which are missing from our map. The bias, caused by the missing zero spacing, is about 3.5 mJy; because it does not affect the visibility of any structures, it has not been added to the maps shown in Figs. 3 and 4. The pattern of the ripple with an amplitude of perhaps 4 mJy is detectable in the contours of the large area map (Fig. 3) particularly moving northeastward from the main ridge of the source where there is first a depression, then a rise, and then another depression. The details of this pattern are not only distorted by the complex source structure but, in turn, the fluctuation limits the measurement of the true large scale features. The amplitude of the ripple is about 1/10 the general brightness of the main ridge so any components near this level are suspect. Fine structure can, of course, be investigated deeper.

To remove as much confusion as possible from the complex map, we have subtracted 19 point sources directly from the $U-V$ plane data before Fourier inversion to make the map. These sources are indicated by asterisks on the maps and in Table 3 which lists all detectable point sources within a 2°.5 field centered at $20^h53^m00^s$ and 31°45′00″. It should be noted that in making the

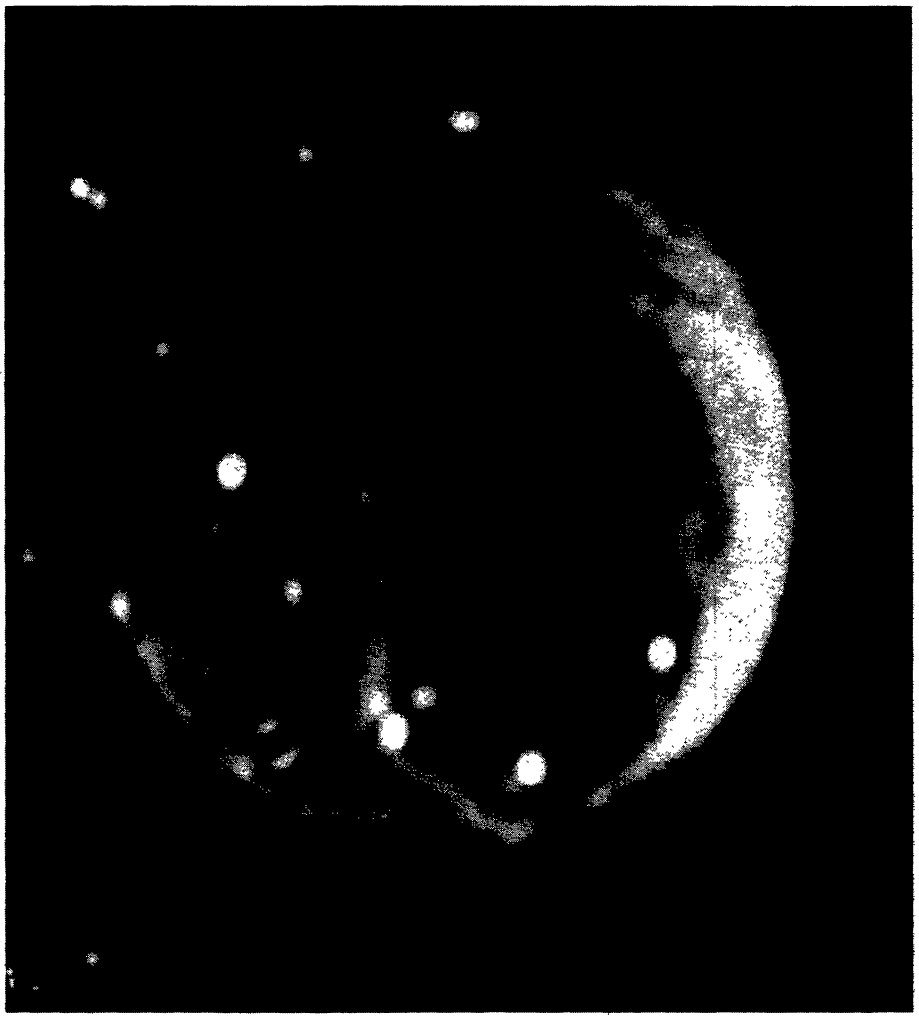

**Fig. 2b**

subtractions, we have removed several sources which are interesting in their own right including the well known object near the center of the SNR, designated CL4 by Keen et al. (1973) (Webster and Ryle, 1975) and the source CL7 which also may be a soft X-ray emitter (Gronenschild, 1978). Their properties can be gotten from the table.

It is difficult to distinguish all the fine details of the SNR in Fig. 3 so we have made two corrections to produce the maps in Fig. 4. First, it was cleaned and second, to extend our information as far westward as possible toward other features of the SNR, we have corrected the maps for the primary beam pattern by multiplying the observed intensity at each point by the inverse of the normalized response of the primary beam at that point. The correction process also increases the apparent noise level near the edges of the map so, although we can see the general shape and intensity of features, it should be borne in mind that the contours are correspondingly uncertain. The multiplying factor at the extreme southwestern point on the final map, Fig. 4, was 25. The contour map in Fig. 4a is superimposed upon a red optical photograph (van den Bergh et al., 1973). The radiophoto in Fig. 4b is from the same radio data except that the point sources have been restored.

No polarization from the SNR was visible above a noise level of 1.5 mJy/beam. That is perhaps 10% of the mean brightness of the shell and 3% of the brightest areas.

## III. Properties of the Remnants

### *A. Shell Characteristics*

Both SNR exhibit significant segments of a complete shell but with sharp gaps and essentially no emission between the segments. The Cygnus Loop also appears to have different radii in different directions, a feature which is even more obvious on maps of the whole remnant with lower resolution (e.g., Keen et al., 1973; DeNoyer, 1974). The individual parts of the shell do not conform to a single surface brightness-diameter (or radius) relation, e.g., $\Sigma_\lambda \alpha R^{-4}$ (Milne, 1979) where $\Sigma_\lambda$ is the radio surface brightness at some given wavelength, $\lambda$, and $R$ is the radius. The southern region of the Cygnus Loop extends perhaps three times further than NGC 6992 but the two arcs have approximately the same surface brightness (DeNoyer, 1974). This vividly demonstrates that unless mass ejection is very irregular, inhomogeneities in the interstellar medium must be controlling the evolution. Major discontinuities appear to have sharp edges and overall sizes of perhaps $^1/_2{}^\circ$ which is considerably smaller than the radius of the remnant. This fact plus the development of the same brightness at different radii would indicate that the emission is probably not caused by a continual sweeping up of accumulated material over the whole volume but is more likely caused by the encountering of significant density fluctuations at different distances from the explosion center.

**Table 2.** Point sources in the field of CTB1

| right ascension (h m s) | declination (° ' ") | flux densities (mJy) 49 cm | 21cm | Notes |
|---|---|---|---|---|
| 23 53 36.05 | 62 17 32.9 | 20.2 | 5.2 | |
| 23 53 41.66 | 62 34 53.0 | 14.6 | 12.3 | |
| 23 53 49.91 | 62 11 55.1 | 24.8 | 4.6 | |
| 23 54 16.06 | 62 33 48.6 | 240.9 | 44.5 | * |
| 23 54 20.31 | 62 33 55.3 | | 82.7 | * |
| 23 55 16.07 | 62 39 25.1 | | 13.3 | |
| 23 55 16.48 | 62 02 59.9 | 107.2 | 41.9 | |
| 23 55 18.38 | 62 01 01.2 | - | 4.3 | a bulge on 50 cm map but not measurable |
| 23 55 18.5 | 61 50 25 | 10.9 | 1.2 | |
| 23 55 33.5 | 61 48 50 | 7.3 | 1.6 | |
| 23 55 45.57 | 61 42 32.3 | 38.8 | 21.2 | |
| 23 55 52.3 | 61 45 32 | 13.5 | 0.7 | (probably extended) |
| 23 56 08.28 | 61 57 31.1 | 88.7 | 48.3 | |
| 23 56 20.89 | 61 52 28.4 | 460.4 | 210.2 | * |
| 23 56 34.0 | 62 28 26 | 50.8 | 4.8 | |
| 23 56 41.0 | 62 28 32 | | 6.8 | |
| 23 56 42.23 | 61 45 54.9 | 28.6 | 20.5 | * |
| 23 56 45.10 | 62 36 37.6 | 112.5 | 42.6 | * |
| 23 56 51.51 | 62 00 42.0 | 21.5 | 10.4 | within SNR-background determination difficult |
| 23 57 03.14 | 61 59 06.5 | 79.3 | 32.5 | |
| 23 57 16.49 | 62 10 14.6 | 12.3 | 8.4 | within SNR |
| 23 57 30.98 | 62 35 49.0 | 15.4 | 2.4 | |
| 23 57 34.71 | 62 25 38.4 | 9.9 | 4.5 | |
| 23 57 40.27 | 62 33 44.6 | (111.8) | 36.8 | not separable at 50 cm from source at $23^h57^m44^s.84$ |
| 23 57 42.14 | 62 26 49.1 | 23.5 | 12.0 | |
| 23 57 44.70 | 62 05 38.7 | 27.5 | 15.9 | |
| 23 57 44.89 | 62 33 21.4 | (111.8) | 26.5 | not separable at 50 cm from source at $23^h57^m40^s.27$ |
| 23 57 46.36 | 62 10 15.4 | 4.1 | 1.6 | |
| 23 57 50.71 | 61 58 24.1 | 680.4 | 271.3 | *extended |
| 23 57 57.31 | 62 15 24.2 | 7 | 3.6 | |
| 23 57 57.9 | 62 15 05 | | 2.7 | |
| 23 58 10.78 | 62 11 18.5 | 120.1 | 32.7 | |
| 23 58 15.17 | 61 46 16.3 | 14.9 | (3.4) | near 21 cm grating ring, uncertain |
| 23 58 16.29 | 62 16 34.2 | 8.3 | 3.8 | |
| 23 58 17.79 | 62 08 39.0 | 13.0 | 8.2 | |
| 23 58 24.23 | 62 33 42.2 | 8.8 | - | 21 cm on grating ring |
| 23 58 40.95 | 62 17 07.4 | 19.2 | 16.4 | |
| 23 59 09.93 | 62 24 22.2 | 44.8 | 12.4 | |
| 23 59 10.23 | 62 47 45.0 | 21.6 | 42.7 | 21 cm on grating ring, uncertain |
| 23 59 19.07 | 62 24 58.8 | 38.0 | 13.6 | |
| 23 59 39.95 | 62 06 54.1 | 21.0 | 7.2 | |
| 23 59 44.39 | 62 35 16.2 | 12.2 | (4.2) | |
| 00 00 04.03 | 61 54 55.8 | 210.2 | (9.0) | 21 cm on grating ring, very uncertain |
| 00 00 18.67 | 62 02 34.6 | 32.7 | - | 21 cm on grating ring |
| 00 00 29.85 | 61 42 45.3 | 9.0 | - | 21 cm too far from field center for reliable flux density |
| 00 00 41.79 | 61 39 41.6 | 29.8 | - | 21 cm too far from field center for reliable flux density |
| 00 00 52.32 | 61 42 57.7 | 5.8 | - | 21 cm too far from field center for reliable flux density |
| 00 00 52.46 | 62 30 52.7 | 18.8 | - | 21 cm too far from field center for reliable flux density |
| 00 00 54.98 | 62 40 09.9 | 6.6 | - | 21 cm too far from field center for reliable flux density |

Despite the brokenness, the emitting zone around the periphery of each source is quite thin. For CTB1, we have made radial cuts from the center of the remnant through the apparent shell and obtained an average radial response at position angles from 90° around through 350°. This response can be well approximated by a uniform shell with a thickness-to-radius ratio of 0.15, very close to the value determined by Willis (1973) with lower resolution data. Although we did not observe the whole Cygnus Loop, we determined a thickness-to-radius ratio of the bright arc NGC 6992/5 of about 0.07, similar to that given by Moffat (1971).

The maps also clearly show that the remnants do not consist of a uniform shell or sheets seen edgewise. This is most obvious in the spur of radio emission in CTB1 running approximately north-south across the center of the remnant at about $23^h57^m17^s$. Toward the south, it apparently twists westward to blend with the main shell emission. On the north there is a suggestion, particularly on the 21-cm radiophoto, that this feature arcs around to join the eastern edge of the shell. Sofue (1978) has suggested that such structures can be created by distortion of hydromagnetic wave fronts interacting with surrounding interstellar clouds.

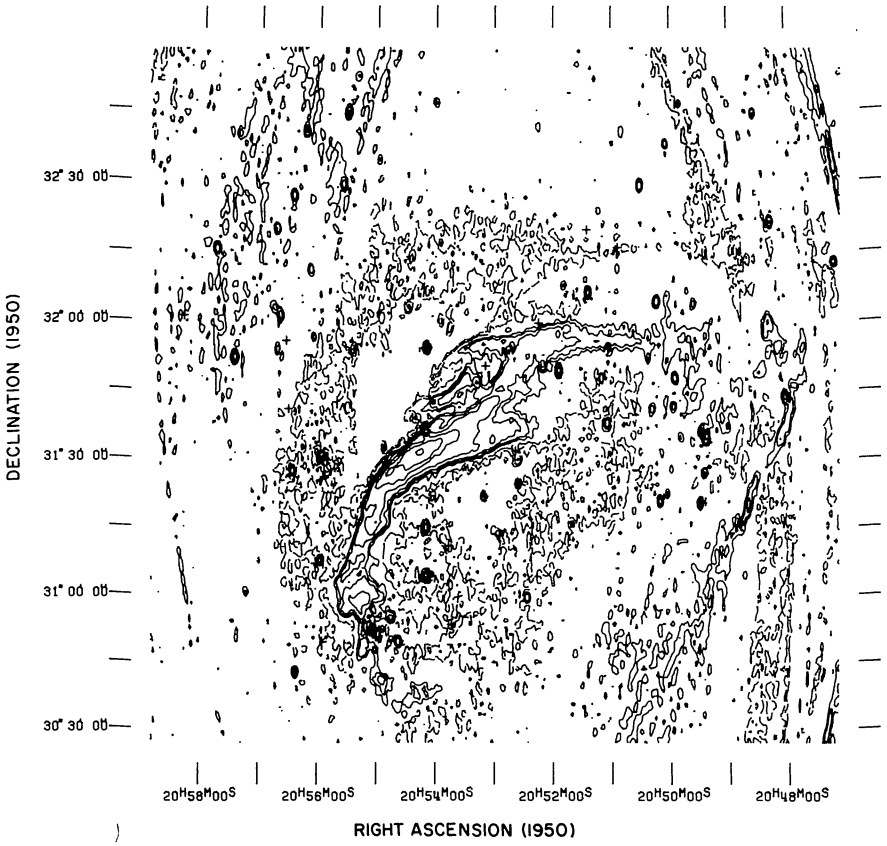


**Fig. 3.** Contour map of the original field of the Cygnus Loop at 50 cm after subtraction of 19 point sources at positions indicates by +'s. The dashed contours indicate negative values. The contour values are −2, 2, 4, 7.5, 15, 30, 50, and 100 mJy/beam area

*B. Comparison with Data in Other Wavelength Ranges*

In both SNR there appears to be a 1–1 correspondence between radio and optical features. To within the limits of our sensitivity and resolution, every feature seen in one wavelength range can be identified in the other and their relative intensities appear to match well. For CTB1, the correlation of the 49-cm emission with the optical was reported previously (Dickel et al., 1977) and the virtually identical map with higher resolution at 21 cm confirms the agreement. In the Cygnus Loop, one bright but very thin optical filament running approximately east-west at about $20^h54^m$ and 31°02′ is not seen in the radio overlay (Fig. 4a) but is hinted at in the radiophoto (Fig. 4b). The faint outer arc to the north of the Cygnus Loop seen in Hα (Gull et al., 1977) and possibly in soft X-rays (Gronenschild, 1978) is faintly visible with the aid of eye integration on the radiophoto (Fig. 4b) but its relative intensity cannot be accurately measured because of the confusion noise mentioned above.

The perfect correspondence indicates that the relativistic particles and magnetic field responsible for the radio synchrotron emission are tied directly to the thermal gas responsible for the optical emission. This characteristic appears to hold for all old SNR (Duin and van der Laan, 1975; Willis, 1973) except Puppis A where the radio and optical appear to have little relation; the reason for the pecularity of Puppis A remains unknown. Although pre HEAO-2 X-ray maps of SNR are of limited resolution, the emission in this wavelength range also appears in good agreement with the general outline of the radio and optical structures (Winkler and Clark, 1974; Rappaport et al., 1979).

In CTB1 the radio filaments appear fatter than the optical ones but for both the Cygnus Loop and CTB1, the form of the radio features resembles that of their optical counterparts. The Cygnus Loop is composed of bright delicate filaments of fairly short length whereas in CTB1, the optical shell appears to consist of more diffuse filaments. We might envision the filaments to be tubes which are cool and relatively dense in the interior where the optical emission is produced but hotter around the outside. The relativistic particles and magnetic field responsible for the non-thermal radio emission are present throughout.

One possible exception to the correlation of radio and optical emission is the wisp of optical nebulosity breaking out from the shell of the Cygnus Loop at $\alpha 20^h54^m26^s$ and $\delta 31°37'00''$. Although a conclusive measurement is hampered by both sensitivity and resolution, there is, if anything, a possible decrease in the radio brightness there.

We should also note that Moffat (1971) reported that the optical filament in the more diffuse southern part of the Cygnus Loop appears to be on the outer edges of the radio shell, a characteristic seen in the much younger Tycho's SNR (Hermann and Dickel, 1973).

*C. Size of the Radiating Regions*

In comparison of the two maps of CTB1, it is immediately obvious that the outer edges are everywhere resolved, even at 49 cm. An actual overlay of the two images, which differ by a factor of $2^1/_2$ in resolution shows no differences greater than the noise level except at the position of the point sources which are larger at 49 cm. Not only are there no spectral index variations across the source but the observed structures are extended enough to be everywhere resolved at both wavelengths. Although there is

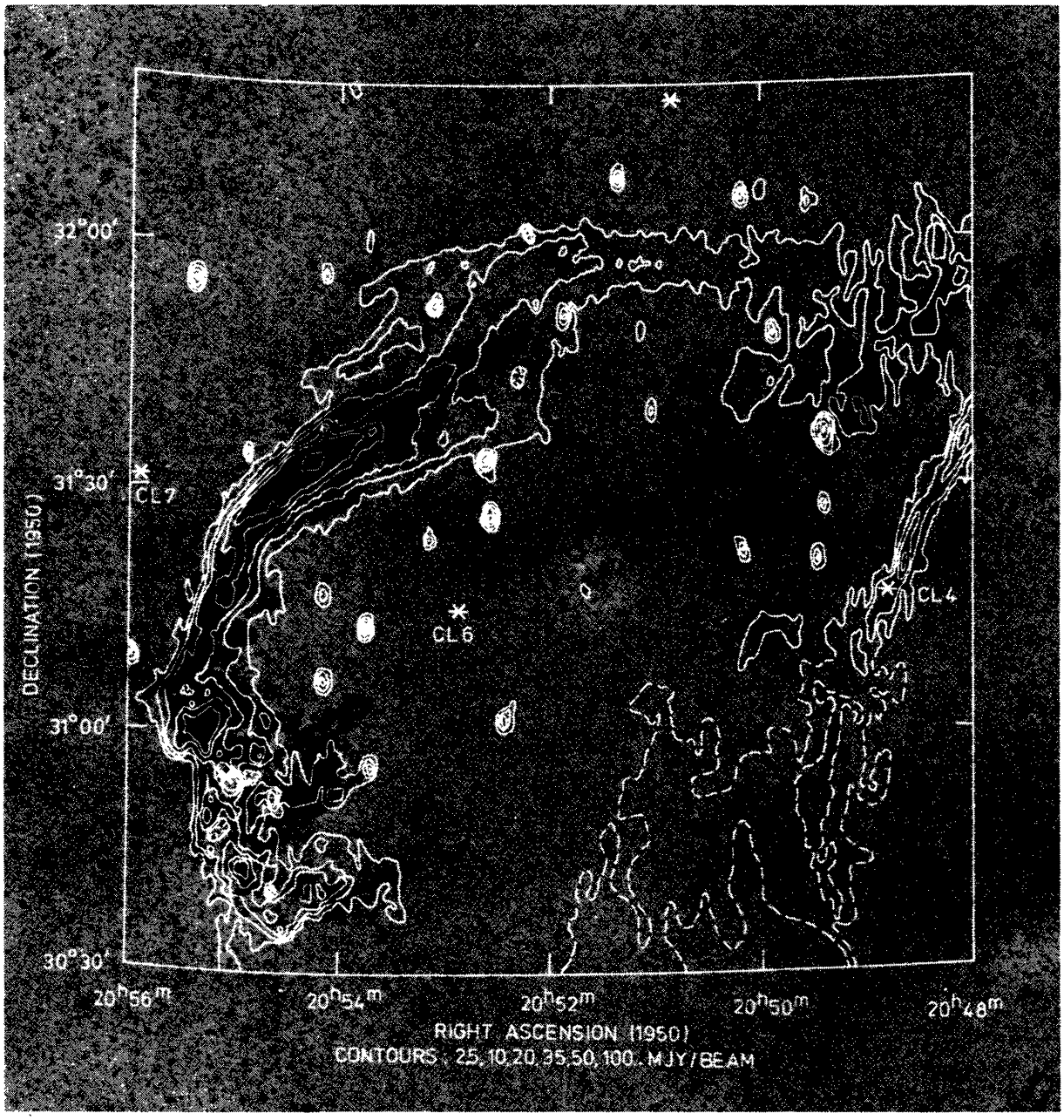


**Fig. 4a**

fine detail visible, the radio emission must arise not behind a sharply defined outer boundary but become increasingly intense over a minimum distance of about 30″. This is true even at the bright western edge of the remnant.

The emission from the Cygnus Loop, on the other hand, has much steeper edges; it does not broaden the beam at all. The apparent gentler gradient in brightness on the outer edge of the shell as it swings around to the north is an artifact of the elliptical beam which has approximately twice the beamwidth in the north-south direction as in the east-west direction. Although the outer edge of the shell is sharp everywhere there is a gradual increase in the emission from the inner to the outer side. This could be the result of superposition of many components along the line of sight through the outside of the shell where the emitting regions are preferentially distributed or caused by greatest emissivity near the shock front on the outer edge.

In order to obtain the physical size of the observed features, we must know the distances to the SNR. For the Cygnus Loop we have adopted the usually assumed values of 770 pc (Minkowski, 1958) which means that 1′ corresponds to 0.22 pc. Thus, the rise in the radio emission at the edges must occur across a distance of less than 0.1 pc.

The distance of CTB1 is very uncertain. The assumption that the remnant lies on Milne's (1979) surface brightness-diameter relation leads to a distance of 5.8 kpc. However, Sato (private communication) has recently found evidence for an incomplete shell of neutral hydrogen possible associated with CTB1 at a radial velocity of $-28\,\mathrm{km\,s^{-1}}$. If this association holds true, then

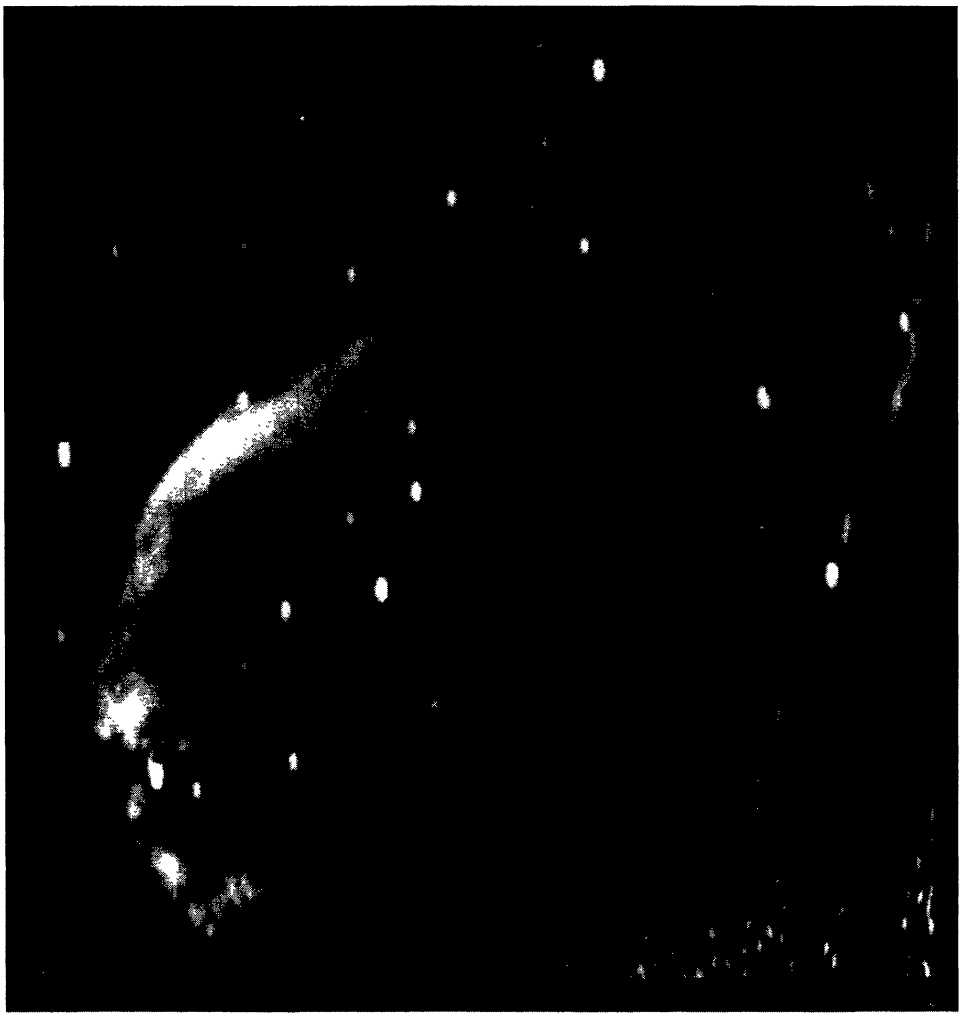

Fig. 4b

**Fig. 4. a** Corrected contour map of part of the Cygnus Loop. This map was produced from Fig. 3 after cleaning and correcting for the attenuation of the primary beam pattern. The positions of subtracted point sources are indicated by asterisks. The shape of the synthesized beam can be seen from the contours of the remaining point sources in the field. The dashed contours are uncertain because of the large noise level in that region of the map caused by the main beam correction. The radio map is superimposed upon a red optical photograph from van den Bergh et al. (1973). **b** Radiophoto of the same region shown in **a** except that the subtracted point sources have been restored

the kinematic distance would be 2.1 kpc. Thus there exists at least a factor of 3 uncertainty in the distance. Because the surface brightness-diameter relation is certainly only statistical and as described above, does not apply accurately even within a single remnant, we shall adopt the kinematic value of the distance. As we are concerned with the minimum size of the radio structure, this closer distance also provides the strongest lower limits to the sizes of the observed features. At 2.1 kpc, 1′ corresponds to 0.61 pc so that the rise in intensity at the edges of CTB1 must occur over a scale greater than 0.3 pc, definitely larger than that in the Cygnus Loop.

## IV. Discussion

### *A. Maintenance of Radio Emission*

Although they have significant structural differences, the two remnants have about the same radio surface brightness. On the other hand, CTB1 is probably about half as large physically so that the luminosity of the Cygnus Loop is significantly greater. Because the luminosity of old SNR is greater than can be accounted for by mere decay of the radiation from the early ejection plus the emission from swept up material (van der Laan, 1962; DeNoyer, 1974), there must be further compression of the accumulated material and/or further acceleration of relativistic particles. Recent comparisons of the intensities of lines from different excited ions of the same element (Woodgate and Lucke, private communication; Miller, 1974) show definite temperature gradients across the shells of several SNR, including the Cygnus Loop, which indicate that the material is still being heated by shocks and progressively cooling away from the shocked region.

The cooling is by radiation of excited atomic lines (Cox, 1972) and to maintain a pressure equilibrium within the shell the gas will contract. This compression will enhance both the magnetic field strength and particle energies causing an increase in the radio emission as suggested by Duin and van der Laan (1975). If the distribution of relativistic particles in a medium is given by a power law of the form:

$$N(E)dE = KE^{-\gamma}dE, \tag{1}$$

where $E$ is the energy of the particles then the ratio of the synchrotron emissivity (of a given volume at a frequency $\nu$) after compression to that before compression is given by

$$\frac{\varepsilon_\nu}{\varepsilon_{\nu_0}} = \frac{K}{K_0}\left(\frac{H}{H_0}\right)^{\frac{\gamma+1}{2}}; \tag{2}$$

**Table 3.** Point sources in the field of the Cygnus Loop

| right ascension $20^h$ m s | declination ° ′ ″ | Flux density (mJy) | Notes |
|---|---|---|---|
| 47 09.77 | 32 12 37.5 | 185 | |
| 48 01.05 | 31 43 52.2 | 136 | |
| 48 16.07 | 32 25 35.1 | 159 | |
| 48 33.20 | 32 44 41.5 | 164 | |
| 48 47.44 | 31 16 10.9 | 418 | * CL4 |
| 49 24.50 | 31 27 47.5 | 25 | |
| 49 25.62 | 31 36 26.2 | 138 | * maybe extended |
| 49 28.93 | 31 21 10.8 | 33 | |
| 49 35.68 | 32 04 29.9 | 16 | |
| 49 54.40 | 31 48 39.2 | 28 | |
| 49 56.05 | 31 42 23.7 | 12 | |
| 50 02.29 | 31 23 34.1 | 10 | |
| 50 04.39 | 32 38 47.3 | 41 | |
| 50 10.22 | 31 21 52.6 | 26 | |
| 50 13.57 | 32 05 12.7 | 32 | |
| 50 18.32 | 31 42 00.8 | 11 | |
| 50 22.33 | 31 53 40.9 | 10 | |
| 50 30.55 | 32 30 04.4 | 58 | |
| 50 53.61 | 32 16 56.4 | 517 | * |
| 51 03.00 | 31 55 12.8 | 76 | * |
| 51 04.45 | 31 39 06.0 | 19 | |
| 51 10.22 | 31 48 53.4 | 9 | |
| 51 24.21 | 32 07 20.3 | 36 | |
| 51 25.58 | 31 20 50.1 | 90 | * |
| 51 53.67 | 31 50 39.2 | 24 | |
| 52 14.25 | 32 00 56.8 | 88 | * |
| 52 26.15 | 31 01 02.7 | 34 | |
| 52 35.28 | 31 25 57.2 | 114 | * |
| 52 38.16 | 31 33 16.8 | 54 | * |
| 52 54.36 | 31 14 44.4 | 427 | * CL6 |
| 53 08.81 | 31 51 44.3 | 51 | * |
| 53 10.37 | 31 23 19.7 | 39 | * |
| 53 43.35 | 30 54 58.7 | 80 | * |
| 53 46.48 | 31 12 21.1 | 103 | * |
| 54 09.44 | 31 55 36.0 | 23 | |
| 54 37.24 | 30 51 05.0 | 61 | |
| 55 01.11 | 30 53 27.8 | 906 | * |
| 55 24.44 | 31 54 57.9 | 40 | * |
| 55 31.02 | 32 45 32.1 | 144 | |
| 55 35.72 | 32 30 20.2 | (52) | on edge of extended feature, uncertain |
| 55 56.40 | 31 30 51.1 | 976 | * CL7 |
| 55 58.21 | 31 08 53.4 | 35 | |
| 56 09.19 | 32 11 54.3 | 21 | |
| 56 14.30 | 32 41 26.8 | 86 | |
| 56 22.16 | 30 43 48.5 | 129 | |
| 56 26.56 | 32 27 37.1 | 71 | |
| 56 27.03 | 31 28 18.6 | 33 | |
| 56 31.17 | 31 41 48.5 | 64 | * |
| 56 34.19 | 31 56 32.0 | 68 | * |
| 56 40.19 | 32 02 04.5 | 37 | |
| 56 42.60 | 31 54 43.2 | 17 | |
| 56 43.71 | 32 20 35.1 | 41 | |
| 57 26.65 | 31 52 40.6 | 97 | |
| 57 45.88 | 32 15 50.7 | 107 | |
| 58 19.41 | 32 01 15.7 | 273 | * |

where $H$ is the magnetic field strength and the subscript 0 refers to original values. In an SNR, the original interstellar medium is first compressed by passage through the shock and then subsequently by the cooling process. During passage through the shock, the actual increase depends upon the orientation of the original interstellar field and particle orbits relative to the propagation direction of the shock. We shall assume that the field is random so that the magnetic field increases in strength by about 2/3 of the factor of 4 density increase in the material. The additional compression of the magnetic field during the cooling phase should be the same as that of the material. Because the compression actually increases the energy of each particle as well as the density, we find that the change in the energy distribution coefficient, $K$, is greater than the density increase. Following Duin and

van der Laan (1975), we assume that the contraction is essentially cylindrical into tubes so that

$$K/K_0=(\varrho/\varrho_0)^{\frac{\gamma+1}{2}}, \quad (3)$$

where $\varrho$ is the density.

To investigate the magnitude of this effect we shall consider the filaments in the Cygnus Loop. Expansion velocities of almost 300 km s$^{-1}$ measured at some positions by Kirshner and Taylor (1976) and the observed X-ray intensity (Stark and Culhane, 1979) are both consistent with a post-shock temperature of $\sim 2\,10^6$ K and density of 2 cm$^{-3}$. This gas can cool to the observed temperature of about $2\,10^4$ K and density of 200 cm$^{-3}$ in the filaments (Parker, 1964, 1967) in somewhat under $10^5$ yr (Savedoff et al., 1967 with faster cooling rates from Cox and Tucker, 1969). This is perhaps twice the generally accepted age of the remnant. The total density enhancement was a factor of 4 from passage through the shock and an additional factor of 100 from the cooling. On the other hand, at some positions just outside features in the Cygnus Loop, DeNoyer (1975) has found clouds of neutral hydrogen with a density of about 5 cm$^{-3}$ and Minkowski (1958) has found some expansion velocities of less than 100 km s$^{-1}$. These numbers would suggest shock temperatures of only about $10^5$ K, a total density enhancement by a factor of 40, and cooling times of a few thousand years. The cooling of this material would quickly leave a large reservoir of neutral gas inside the remnant which is not seen in the Cygnus Loop (DeNoyer, 1975), so not much of the remnant can already have intercepted such dense clouds. An intermediate value to represent the conditions in the whole remnant with about the correct cooling time scale would provide a total density enhancement (shock plus cooling) of about a factor of 100. Finally, the spectral index of the Cygnus Loop below 1 GHz is $-0.38$ (DeNoyer, 1974) which corresponds to a $\gamma$ of 1.76. Substitution of these numbers into Eqs. (2) and (3) gives a volume emissivity of the filaments which is $2\,10^5$ times that of the galactic background. The galaxy has a mean volume emissivity of $3\,10^{-39}$ erg s$^{-1}$ Hz$^{-1}$ cm$^{-3}$ at a wavelength of 49 cm (Baldwin, 1967) and so we would expect a value of about $6\,10^{-34}$ erg s$^{-1}$ Hz$^{-1}$ cm$^{-3}$ in the filaments. If each filament is cylindrical with a diameter of 0.1 pc then our mean observed flux density of about 20 mJy/beam in this region corresponds to an emissivity of $3\,10^{-34}$ erg s$^{-1}$ Hz$^{-1}$ cm$^{-3}$, within a factor of 2 of the predicted value.

The compression by a factor of 100 also means that 1/100 of the SNR should be filled by filaments, a not unreasonable value from visible inspection. Furthermore, assuming a mean path length of 30 pc through the SNR we find the compression-enhanced emission from 1/100 the volume should be $\sim 300$ Jy which is the value observed for the integrated flux density of the Cygnus Loop at 49 cm by DeNoyer (1974). These fortuitously close agreements do not, of course, take into account the actual density fluctuations, the possibility of multiple filaments in the beam, etc. but the results clearly show that this proposed mechanism can indeed account for the observed radio emission.

### B. *Spectrum*

A remnant with this great emissivity will lose a significant amount of energy in synchrotron radiation, the most energetic particles losing their energy the most rapidly. Such a process will thus create a "kink" in the radio spectrum such that the flux density above some break frequency will decrease more rapidly with increasing frequency than it does below the break. As more particles radiate away their energy, the break frequency will move downward with time according to the formula (Kardashev, 1962):

$$\nu_B=0.34H^{-3}t^{-2}, \quad (4)$$

where $\nu_B$ is the break frequency in GHz, $H$ the magnetic field strength in gauss, and $t$ the time in years. The Cygnus Loop appears to have a kink of this nature in its spectrum with a break frequency near 1 GHz (DeNoyer, 1974; Kundu and Becker, 1972). A compression of the interstellar magnetic field by the mean factor of about 75 will produce a magnetic field strength within the filaments of about $2\,10^{-4}$ Gauss (e.g., Whiteoak, 1974). These numbers give a time scale in Eq. (4) of $2\,10^5$ yr, several times the apparent age of the Cygnus Loop but there are factors which might shorten the time scale. If, after compression, part of the shell encounters a less dense medium then it may then reexpand, quickly reducing the particle energy. Under these conditions the break frequency will be given by:

$$\nu_B=0.34H^{-3}t^{-2}\left[\frac{4}{t^4\left(\frac{1}{t_0^4}-\frac{1}{t^4}\right)}\right]^2, \quad (5)$$

where $t_0$ is the time since the expansion began. A value of 2 for $t/t_0$ reduces the time for the break frequency to reach 1 GHz by a factor of 14. Thus the great range of conditions encountered by the Cygnus Loop, as already mentioned above, could allow the kink in the spectrum to be accounted for by the loss of particles at the highest energy. Such a process would predict that the spectral break would occur at different frequencies at different positions in the remnant. Accurate spectral index maps over a broad frequency range covering the whole source are needed to test this hypothesis.

Observations of other SNR are not inconsistent with this result. Although for many remnants, including CTB1, data above 2.7 GHz are either non-existent or poor, only one other source, HB9, exhibits a break in its spectrum (DeNoyer, 1974). Most of the others have fairly flat spectra so the break frequency cannot be below the observable range. As most remnants are probably younger than the Cygnus Loop and have lower luminosities, the presence of a kink within the observable range of the spectrum should be rare.

### C. *Comparison of the Cygnus Loop and* CTB1

The strong X-ray emission and high radio luminosity plus the fine scale of the observed filaments in the Cygnus Loop argue that there has been a more significant shock interaction with the surrounding medium in this remnant than in CTB1. As mentioned above, CTB1 has probably gone off in the vicinity of an H II region (Willis and Dickel, 1971) which would quickly impede the expansion and allow only a small increase in temperature behind the shock. The cooling process will therefore entail less drastic compression and stratification in the remnant which can account for the emissivity and morphology differences. Because the cooling from the low temperature will proceed faster there may be some neutral hydrogen within the shell of CTB1. Thus the two old SNR, the Cygnus Loop and CTB1, have evolved in a similar manner and the differences between tham can likely be attributed to different ambient conditions in the medium surrounding each.

In summary, the nearly perfect 1–1 correspondence of radio and optical features in old SNR means that the two kinds of emission must arise in the same vicinity although the radio features appear somewhat larger. The filaments can be created by

thermal instabilities in the initially hot gas behind the shock fronts. Compression of the cooling gas perpendicular to the magnetic field will produce both the optical spectrum and the enhanced radio emission.

*Acknowledgements.* It is a pleasure to thank H. van der Laan for continued stimulation throughout the course of this investigation. Thanks are also due to L. DeNoyer, R. Strom, B. van Leer, C. Norman, E. Gronenschild, T. Gull, and T. Mouschovias for valuable discussions. We appreciate the comments of a referee who led us to rethink some of the interpretation. R. Harten, P. Katgert, T. Hoekema, L. Zuiderduin, and D. Wells have helped with the data presentation. The WSRT is operated by the Netherlands Foundation for Radio Astronomy (SRZM) with financial support of the Netherlands Organization for Advancement of Pure Research (ZWO). JRD gratefully acknowledges a travel award to Leiden by the Netherlands-America Commission for Educational Exchange under the Fulbright Hays Program.

## References

Baldwin, J.E.: 1967, in *Radio Astronomy and the Galactic System*, IAU *Symp.* No. 31, ed. by H. van Woerden, New York: Academic Press, p. 337
van den Bergh, S., Marscher, A.P., Terzian, Y.: 1973, *Astrophys. J. Suppl.* **26**, 19
Cox, D.P.: 1972, *Astrophys. J.* **178**, 143, 1959, 169
Cox, D.P., Tucker, W.H.: 1969, *Astrophys. J.* **157**, 1157
DeNoyer, L.K.: 1974, *Astron. J.* **79**, 1253
DeNoyer, L.K.: 1975, *Astrophys. J.* **196**, 479
Dickel, J.R.: 1978, *Astrophys. Letters* **19**, 115
Dickel, J.R., Wells, D.C., Gull, T.R., Bergh, S. van den, Willis, A.G.: 1977, in *Supernovae*, ed. by D.N. Schramm, Dordrecht, Reidel, p. 63
Duin, R.M., van der Laan, H.: 1975, *Astron. Astrophys.* **40**, 111
Gronenschild, E.H.B.M.: 1978, submitted to *Astron. Astrophys.*
Gronenschild, E.H.B.M.: 1979, *Astron. Astrophys.* **77**, 53
Gull, T.R., Parker, R.A.R., Kirshner, R.P.: 1977, in *Supernovae*, ed. by D.N. Schramm, Dordrecht, Reidel, p. 71
Hermann, B.R., Dickel, J.R.: 1973, *Astron. J.* **78**, 879
Högbom, J.A., Brouw, W.N.: 1974, *Astron. Astrophys.* **33**, 289
Kardashev, N.S.: 1962, *Soviet Astron. J.* **6**, 317
Keen, N.H., Wilson, W.E., Haslam, C.G.T., Graham, D.A., Thomasson, P.: 1973, *Astron. Astrophys.* **28**, 197
Kirshner, R.P., Taylor, R.: 1976, *Astrophys. J. Letters* **208**, L83
Kundu, M.R., Becker, R.H. 1972, *Astron. J.* **77**, 459
van der Laan, H.: 1962, *Monthly Notices Roy. Astron. Soc.* **124**, 179
Miller, J.S.: 1974, *Astrophys. J.* **189**, 239
Milne, D.K.: 1979, *Australian. J. Phys.* **32**, 83
Minkowski, R.: 1958, *Rev. Mod. Phys.* **30**, 1048
Moffat, P.H.: 1971, *Monthly Notices Roy. Astron. Soc.* **153**, 401
Parker, R.A.R.: 1964, *Astrophys. J.* **139**, 493
Parker, R.A.R.: 1967, *Astrophys. J.* **149**, 363
Rappaport, S., Petre, R., Kayat, M., Evans, K., Smith, G., Levine, A.: 1979, *Astrophys. J.* **227**, 285
Savedoff, M.P., Hovenier, J.W., van Leer, B.: 1967, *Bull. Astron. Inst. Neth.* **19**, 107
Sofue, Y.: 1978, *Astron. Astrophys.* **67**, 409
Stark, J.P.W., Culhane, J.L.: 1978 (preprint)
Velusamy, T., Kundu, M.R.: 1974, *Astron. Astrophys.* **32**, 375
Webster, A., Ryle, M.: 1975, *Monthly Notices Roy. Astron. Soc.* **175**, 95
Whiteoak, J.B.: 1974, in *Galactic Radio Astronomy*, IAU *Symp.* No. 60, ed. by F.J. Kerr and S.C. Simonson, III, Dordrecht, Reidel, p. 137
Winkler, P.F., Clark, G.W.: 1974, *Astrophys. J. Letters* **191**, L67
Willis, A.G.: 1973, *Astron. Astrophys.* **26**, 237
Willis, A.G., Dickel, J.R.: 1971, *Astrophys. Letters* **8**, 203